Enhanced Electrocatalytic Performance for Overall Water Splitting: Exploring Heterojunctions and Vacancy-Engineered Nanosheets

Dexin Yu,[#a] Yifan Zhang,[#a] Jun Wu,[*a] Feng Zhang[*a] and Fengyu Qu[a]

[a]*Key Laboratory of Photochemical Biomaterials and Energy Storage Materials, Harbin Normal University, Harbin 150025, P. R. China*

**Corresponding authors: Feng Zhang (E-mail: zhangfeng@hrbnu.edu.cn) and Jun Wu (wujun@hrbnu.edu.cn)*

[#]*These authors contributed equally to this work.*

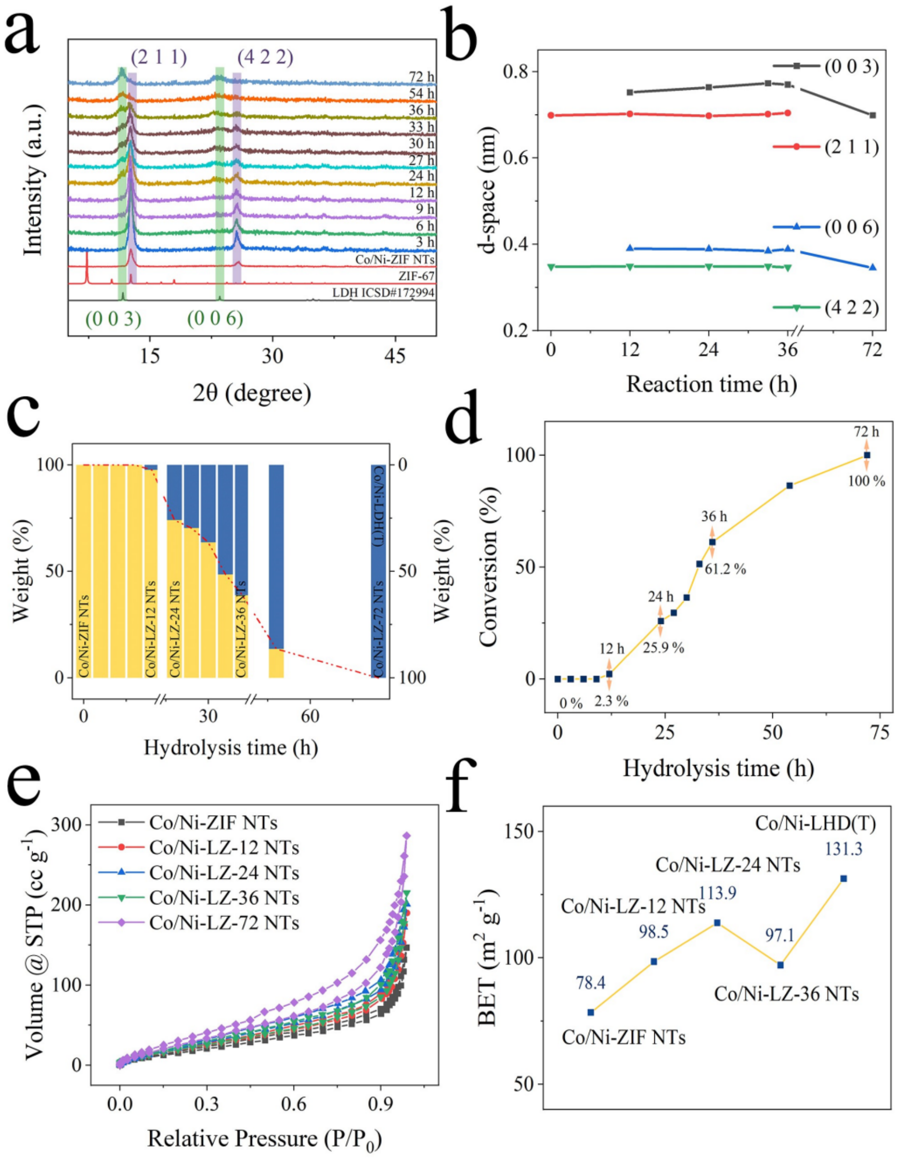

Fig. S1 The PXRD patterns (**a**), the variation of the d-place (**b**), the weight (Wt%) of each phase (**c**), the translate conversion of Co/Ni-ZIF NTs (**d**) in Co/Ni-ZIF NTs and its time transformed derivatives; and the surface areas comparison (**e** and **f**) among the Co/Ni-ZIF NTs and its main derivatives.

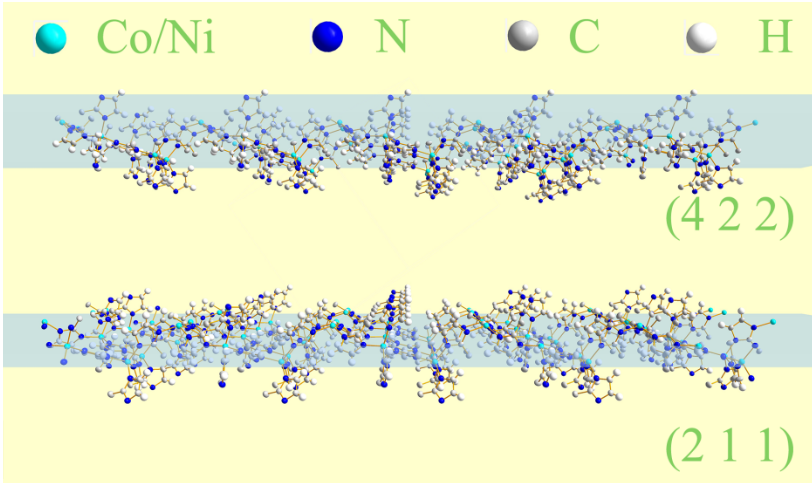

Fig. S2 The specific lattice planes (211) and (422) of Co/Ni-ZIF-67.

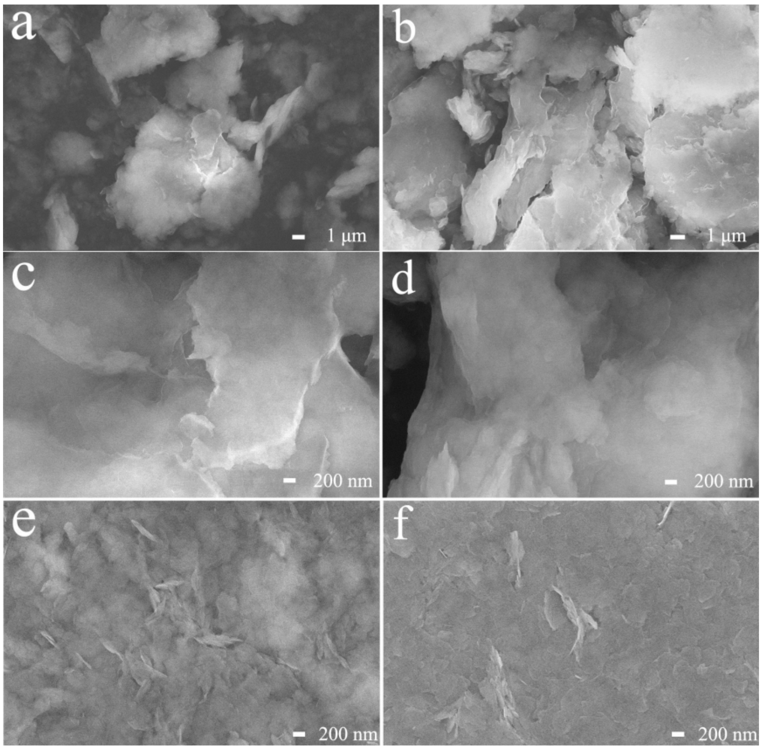

Fig. S3 SEM images of Co/Ni-LZ-24 (**a** and **c**) and Co/Ni-LZ-36 (**b** and **d**). SEM images of Co/Ni-LZ-24 (**e**) and Co/Ni-LZ-72 (**f**) NTs dispersed on silicon.

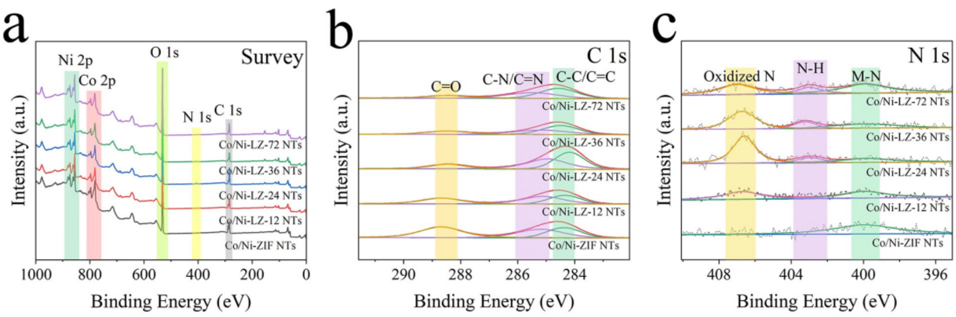

Fig. S4 The survey XPS spectra (**a**) and the high-resolution spectra of C 1s (**b**) and N 1s (**c**) in Co/Ni-ZIF and Co/Ni-LZ-t.

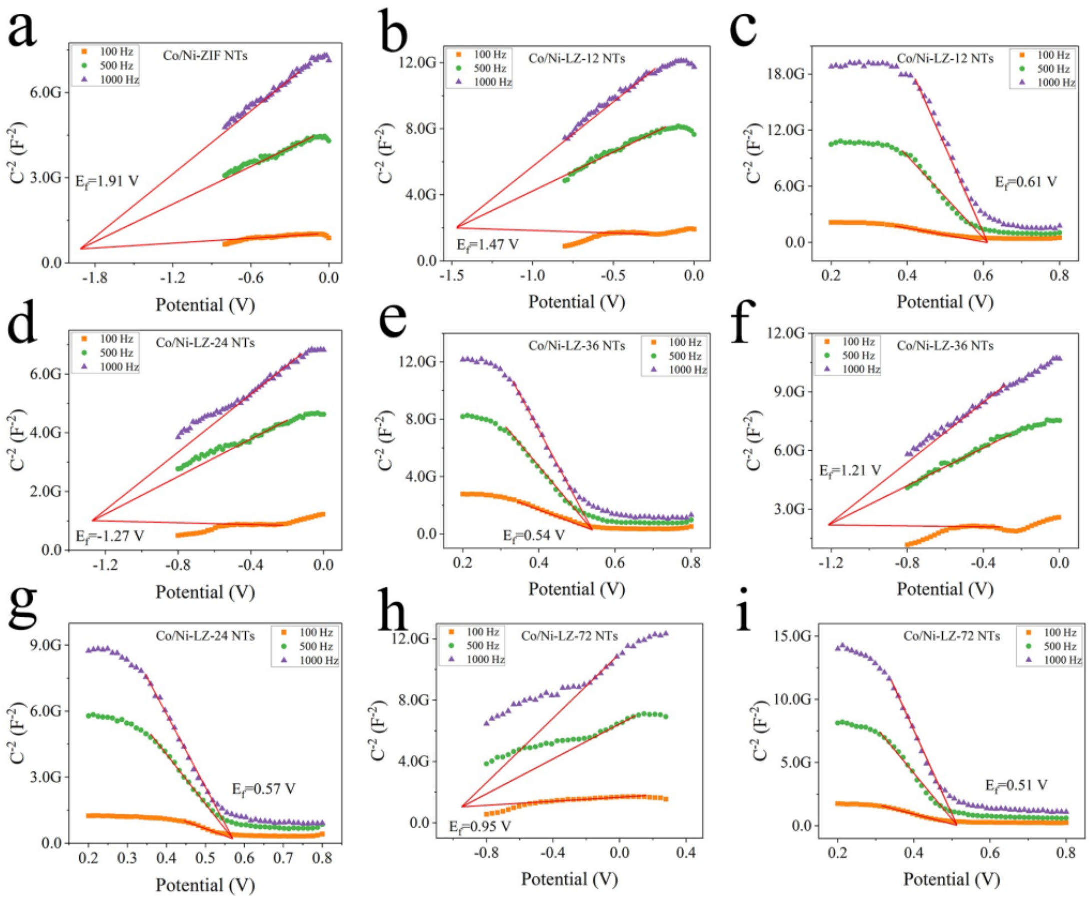

Fig. S5 The Mott-Schottky plots of Co/Ni-ZIF NTs (**a**), Co/Ni-LZ-t NTs(**b** to **g**) and Co/Ni@LDH(T) (**h** and **i**), respectively at different frequencies (100, 500 and 1000 Hz)

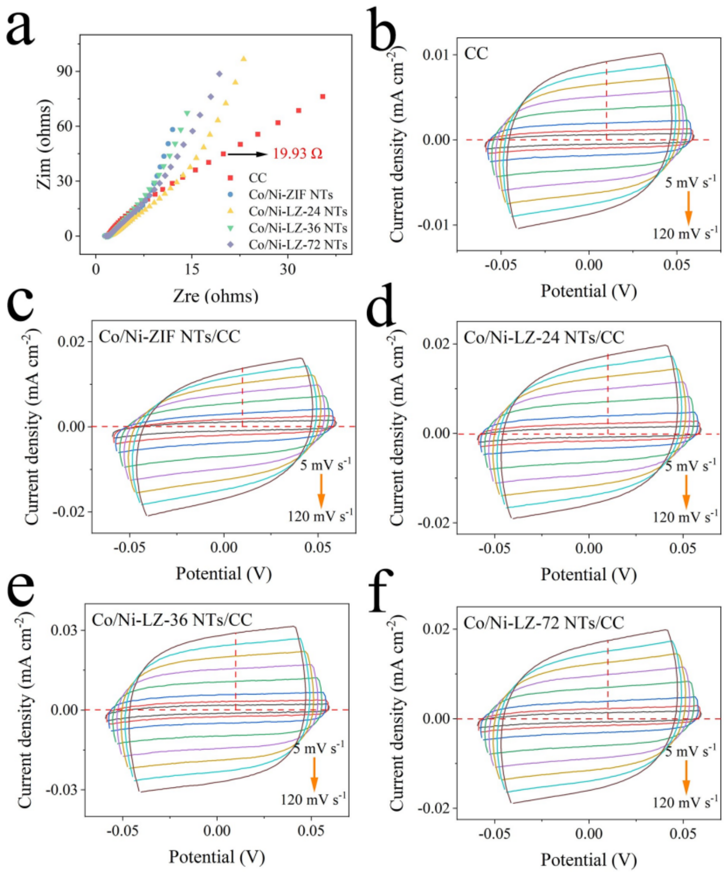

Fig. S6 EIS (**a**) and CV curves in a non-Faradaic region (**b-f**) of CC (**b**), Co/Ni-ZIF NTs/CC (**c**) Co/Ni-LZ-24 NTs/CC (**d**), Co/Ni-LZ-36 NTs/CC (**e**) and Co/Ni@LDH(T)/CC (**f**) at 5 to 120 mV s^{-1}.

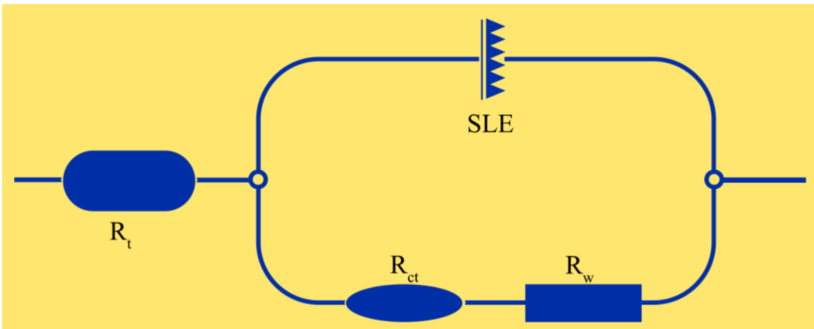

Fig. S7 The Randles equivalent circuit diagram including solution resistance (R_s), charge-transfer resistance (R_{ct}), Warburg impedance (R_w), and the simulated electrodes (SLE).

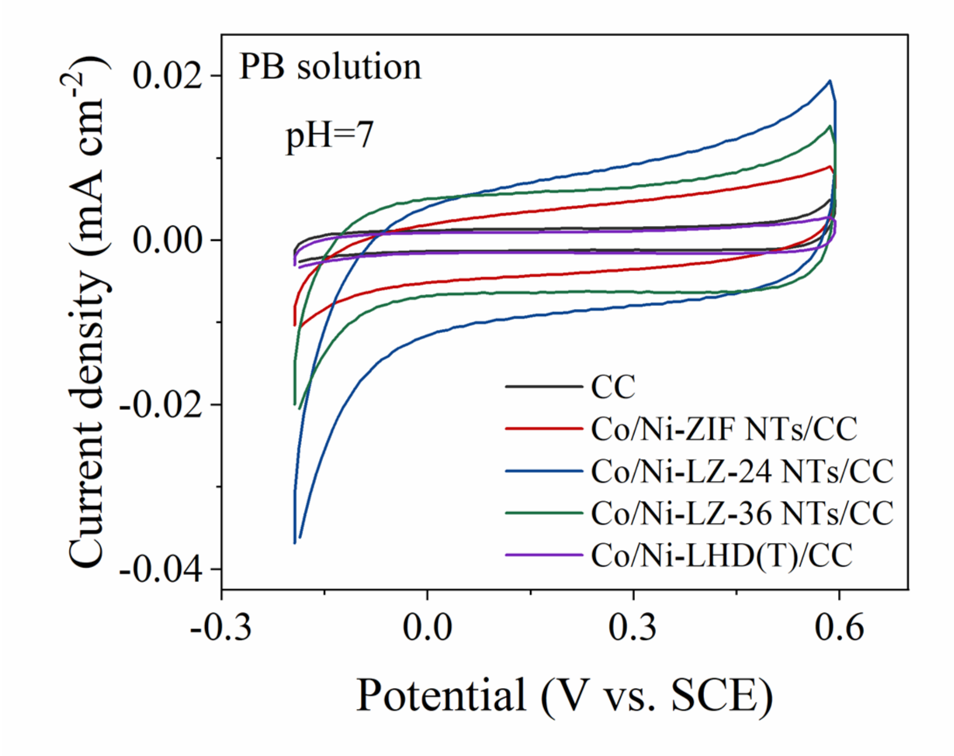

Fig. S8 CVs curves of different electrodes in PB solutions (0.1 M, pH=7.0)

Table S1 The details information of different elements in the high-resolution XPS spectra.

Materials	Binding energy (eV) Co/Ni-ZIF	Co/Ni-LZ-12	Co/Ni-LZ-24	Co/Ni-LZ-36	Co/Ni-LZ-72	Peak type	Ref.
C 1s	284.4	284.4	284.2	284.5	284.6	C-C/C=C	
	285.2	285.1	285.0	285.2	285.5	C-N/C=N	S1
	288.7	288.7	288.4	288.5	288.5	C=O	
N 1s	399.9	399.9	399.8	399.9	399.9	M-N	S1
			402.3	403.2	403.0	graphitic-N	S2
		406.7	406.6	406.7	407.0	oxidized N	S3
O 1s	530.9	530.7	530.7	530.7	530.8	M-O	S4, S5
	531.6	531.5	531.4	531.5	531.7	O_V	S4-S6
	532.4	532.3	532.3	532.3	532.6	adsorbed	S4

						water	
Co 2p	780.7	780.7	780.7	780.7	780.8	Co^{3+} $2p_{3/2}$	S7-S8
	782.0	782.0	782.0	782.0	782.1	Co^{2+} $2p_{3/2}$	
	786.0	786.0	786.0	786.0	786.0	Sat. $2p_{3/2}$	
	796.5	796.5	796.5	796.5	796.6	Co^{3+} $2p_{1/2}$	
	797.8	797.8	797.8	797.8	798.0	Co^{2+} $2p_{1/2}$	
	803.0	803.0	803.0	803.0	803.0	Sat. $2p_{1/2}$	
Ni 2p	856.1	856.0	855.8	855.9	856.3	Ni^{2+} $2p_{3/2}$	S9-S11
	861.9	861.9	861.4	861.7	862.1	Sat. $2p_{3/2}$	
	873.9	873.6	873.4	873.5	874.0	Ni^{2+} $2p_{1/2}$	
	880.1	879.7	879.8	879.7	880.1	Sat. $2p_{1/2}$	

Table S2 The content of each element of all the prepared materials.

Element	Peak-type	Element content				
		Co/Ni-ZIF	Co/Ni-LZ-12	Co/Ni-LZ-24	Co/Ni-LZ-36	Co/Ni-LZ-72
C 1s	C-C/C=C	27.3	31.2	43.1	45.0	46.4
	C-N/C=N	32.9	39.9	41.2	34.7	36.4
	C=O	39.8	28.8	15.6	20.3	17.2
N 1s	M-N	32.9	33.7	36.1	35.5	33.5
	graphitic-N	38.0	36.0	34.7	34.7	34.2
	oxidized N	29.1	30.2	29.2	29.8	32.3
O 1s	M-O	100.0	50.6	21.0	27.9	44.7
	O_V	0.0	0.0	21.0	15.7	17.6
	adsorbed water	0.0	49.4	58.0	56.4	37.7
Co 2p	Co^{3+} $2p_{3/2}$	11.5	22.3	15.3	12.3	10.1

	Co^{2+} $2p_{3/2}$	18.0	22.3	20.5	22.8	21.5
	Sat. $2p_{3/2}$	46.3	22.3	40.2	40.4	46.3
	Co^{3+} $2p_{1/2}$	3.6	8.1	7.3	6.2	4.5
	Co^{2+} $2p_{1/2}$	9.6	8.1	7.6	7.9	9.1
	Sat. $2p_{1/2}$	11.0	16.9	9.1	10.4	8.6
Ni 2p	Ni^{2+} $2p_{3/2}$	30.0	28.6	26.5	26.7	28.4
	Sat. $2p_{3/2}$	30.0	34.9	34.8	34.7	33.4
	Ni^{2+} $2p_{1/2}$	21.7	16.5	19.1	19.2	20.4
	Sat. $2p_{1/2}$	18.3	20.1	19.6	19.4	17.8

Table S3 The semiconductor type and the value of E_f in materials

Materials	Semiconductor Type	E_f (n-type)	E_f (p-type)
Co/Ni-ZIF-67 NTs	n	1.91 eV	/
Co/Ni-LZ-12 NTs	p-n	1.47 eV	0.61 eV
Co/Ni-LZ-24 NTs	p-n	1.27 eV	0.57 eV
Co/Ni-LZ-36 NTs	p-n	1.21 eV	0.54 eV
Co/Ni-LZ-72 NTs	p-n	0.95 eV	0.51 eV

Table S4 The value of resistance, C_{dl} and EASA with different value of C_s

Electrodes	R (Ω)	C_{dl} (mF cm^{-2})	EASA (cm^2)		
			C_s (μF cm^{-2})		
			20	40	60
CC	19.93	0.075	3.76	1.88	1.25
Co/Ni-ZIF-67 NTs/CC	2.35	0.11	5.57	2.78	1.86
Co/Ni-LZ-24 NTs/CC	2.13	0.14	7.08	3.54	2.36
Co/Ni-LZ-36 NTs/CC	1.97	0.24	11.82	5.91	3.94
Co/Ni-LZ-72 NTs/CC	1.88	0.14	7.06	3.53	2.35

Table S5 The overpotentials (η) and Tafel slopes of CC, Co/Ni-ZIF NTs/CC and Co/Ni-LZ-t NTs/CC.

Electrodes	HER		OER	
	η(V)	Tafel slope (mV dec^{-1})	η (V)	Tafel slope (mV dec^{-1})
CC	241.76	381.72	488.49	35.80
Co/Ni-ZIF NTs/CC	119.60	43.54	301.48	32.88
Co/Ni-LZ-24 NTs/CC	80.50	19.88	297.49	36.22
Co/Ni-LZ-36 NTs/CC	100.90	52.81	289.59	28.59
Co/Ni-LZ-72 NTs/CC	97.60	63.79	295.34	40.37

Table S6 Some catalytic parameters in different electrodes.

Electrodes	Q_A (×10^3, Coulombs)	OER a (×10^9, moles)	j (mA cm^{-2}, η=0.4 V	TOF (s^{-1})	HER a (×10^9, moles)	j (mA cm^{-2}, η=-0.15 V	TOF (s^{-1})
Co/Ni-ZIF NTs/CC	2.19	5.67	3.46	1.58	11.3	7.10	3.25
Co/Ni-LZ-12 NTs/CC	5.93	15.4	74.08	12.49	30.7	11.55	1.95
Co/Ni-LZ-24 NTs/CC	13.11	34	85.54	6.53	67.9	13.70	1.04
Co/Ni-LZ-36 NTs/CC	10.05	26	92.09	9.16	52.1	12.70	1.26
Co/Ni-LZ-72 NTs/CC	2.16	5.59	91.18	42.26	11.2	12.47	5.78

Table S7 The comparison of catalytic performances in three-electrode and two-electrode system.

Electrodes	$\eta_{(HER)}$ (mV)	$\eta_{(OER)}$ (mV)	cell voltage (10 mA cm^{-2})	Ref.
Ni-CoP/Co2P-NC	117	/	1.59	S12
Hy-Ni-CoP/Co2P-NC	/	272		
Dual vacancies doped MnO_2	59	260	1.55	S13
CuO-CoZn-LDH/CF	124	194	1.55	S14
Co-N-CS/N-HCP-CC	66	248	1.545	S1
Pt/C-CC‖IrO_2-CC	/	/	1.592 V	
CoFe-NiFe/ NF	160	240	1.59	S15
Co/Ni-LZ-24 NTs	80.5	/	1.59	This work
Co/Ni-LZ-36 NTs	/	289.6		

Reference

S1. Chen, Z.; Ha, Y.; Jia, H.; Yan, X.; Chen, M.; Liu, M.; Wu, R., Oriented Transformation of Co-LDH into 2D/3D ZIF-67 to Achieve Co–N–C Hybrids for Efficient Overall Water Splitting. *Advanced Energy Materials,* 2019, **9(19)**, 1803918.

S2. Huang, J.; Sementa, L.; Liu, Z.; Barcaro, G.; Feng, M.; Liu, E.; Jiao, L.; Xu, M.; Leshchev, D.; Lee, S.-J.; Li, M.; Wan, C.; Zhu, E.; Liu, Y.; Peng, B.; Duan, X.; Goddard, W. A.; Fortunelli, A.; Jia, Q.; Huang, Y., Experimental Sabatier plot for predictive design of active and stable Pt-alloy oxygen reduction reaction catalysts. *Nature Catalysis,* 2022, **5(6)**, 513-523.

S3. Liu, Y.; Li, C.; Loubidi, M.; Wang, D.; Zhou, L.; Niu, S.; Liu, Q.; Huo, J., Increasing exposure of atomically dispersed Ni sites via constructing hierarchically porous supports for enhanced electrochemical CO_2 reduction. *Chemical Engineering Journal,* 2021, **426**, 131414.

S4. Tahir, M. U.; Arshad, H.; Zhang, H.; Hou, Z.; Wang, J.; Yang, C.; Su, X., Room temperature and aqueous synthesis of bimetallic ZIF derived CoNi layered double hydroxides and their applications in asymmetric supercapacitors. *Journal of Colloid and Interface Science,* 2020, **579**, 195-204.

S5. Xie, Y.; Zhou, Z.; Yang, N.; Zhao, G., An Overall Reaction Integrated with Highly Selective Oxidation of 5-Hydroxymethylfurfural and Efficient Hydrogen Evolution. *Advanced Functional Materials,* 2021, **31**(**34**), 2102886.

S6. Zhu, B.; Qin, Y.; Du, J.; Zhang, F.; Lei, X., Ammonia Etching to Generate Oxygen Vacancies on $CuMn_2O_4$ for Highly Efficient Electrocatalytic Oxidation of 5-Hydroxymethylfurfural. *ACS Sustainable Chemistry & Engineering,* 2021, **9(35)**, 11790-11797.

S7. Chen, M.; Wang, N.; Wang, X.; Zhou, Y.; Zhu, L., Enhanced degradation of tetrabromobisphenol A by magnetic Fe3O4@ZIF-67 composites as a heterogeneous Fenton-like catalyst. *Chemical Engineering Journal,* 2021, **413**, 127539.

S8. Li, J.; Li, F.; Liao, J.; Li, H.; Dang, D.; Liu, Q.; Peng, H.-J., Scalable Construction of Hollow Multishell Co_3O_4 with Mitigated Interface Reconstruction for Efficient Lithium Storage. *Advanced Materials Interfaces,* 2020, **7**(**14**), 2000667.

S9. Kale, A. M.; Manikandan, R.; Justin Raj, C.; Dennyson Savariraj, A.; Voz, C.; Kim, B. C., Protonated nickel 2-methylimidazole framework as an advanced electrode material for high-performance hybrid supercapacitor. *Materials Today Energy,* 2021, **21**, 100736.

S10. Shih, Y.-J.; Lin, P.-Y.; Wu, Z.-L., Catalytic oxidation and deionization of nitrite and nitrate ions using mesoporous carbon-supported nano-flaky cobalt and nickel oxyhydroxides. *Journal of Colloid and Interface Science,* 2022, **611**, 265-277.

S11. Wang, Z.; Xu, L.; Huang, F.; Qu, L.; Li, J.; Owusu, K. A.; Liu, Z.; Lin, Z.; Xiang, B.; Liu, X.; Zhao, K.; Liao, X.; Yang, W.; Cheng, Y.-B.; Mai, L., Copper–Nickel

Nitride Nanosheets as Efficient Bifunctional Catalysts for Hydrazine-Assisted Electrolytic Hydrogen Production. *Advanced Energy Materials,* 2019, **9**(**21**), 1900390.

S12. Chu, H.; Feng, P.; Jin, B.; Ye, G.; Cui, S.; Zheng, M.; Zhang, G.-X.; Yang, M., In-situ release of phosphorus combined with rapid surface reconstruction for Co–Ni bimetallic phosphides boosting efficient overall water splitting. *Chemical Engineering Journal,* 2022, **433**, 133523.

S13. Liu, Y.; Bui, H. T. D.; Jadhav, A. R.; Yang, T.; Saqlain, S.; Luo, Y.; Yu, J.; Kumar, A.; Wang, H.; Wang, L.; Bui, V. Q.; Kim, M. G.; Kim, Y. D.; Lee, H., Revealing the Synergy of Cation and Anion Vacancies on Improving Overall Water Splitting Kinetics. *Advanced Functional Materials,* 2021, **31**(**21**), 2010718.

S14. Yin, L.; Du, X.; Di, C.; Wang, M.; Su, K.; Li, Z., In-situ transformation obtained defect-rich porous hollow CuO@CoZn-LDH nanoarrays as self-supported electrode for highly efficient overall water splitting. *Chemical Engineering Journal,* 2021, **414**, 128809.

S15. Yang, R.; Zhou, Y.; Xing, Y.; Li, D.; Jiang, D.; Chen, M.; Shi, W.; Yuan, S., Synergistic coupling of CoFe-LDH arrays with NiFe-LDH nanosheet for highly efficient overall water splitting in alkaline media. *Applied Catalysis B: Environmental,* 2019, **253**, 131-139.